NASA TECHNICAL MEMORANDUM

NASA TM X-1579

NASA TM X-1579

EXPERIMENTAL INVESTIGATION OF MERCURY PROPELLANT FEED ISOLATORS FOR KAUFMAN THRUSTERS

by Shigeo Nakanishi

Lewis Research Center

Cleveland, Ohio

NATIONAL AERONAUTICS AND SPACE ADMINISTRATION • WASHINGTON, D. C. • MAY 1968

NASA TM X-1579

EXPERIMENTAL INVESTIGATION OF MERCURY PROPELLANT FEED ISOLATORS FOR KAUFMAN THRUSTERS

By Shigeo Nakanishi

Lewis Research Center
Cleveland, Ohio

NATIONAL AERONAUTICS AND SPACE ADMINISTRATION

For sale by the Clearinghouse for Federal Scientific and Technical Information
Springfield, Virginia 22151 – CFSTI price $3.00

ABSTRACT

Electrical breakdown voltages and leakage currents were experimentally determined for seven high-voltage isolator configurations designed for the mercury propellant feed system of a SERT II type Kaufman ion thruster. An isolator containing 40 insulated segments experienced no breakdown up to 5000 volts, but leakage current at 3000 volts was about 0.10 milliampere. A configuration utilizing a long propellant flow passage and large recombination surface areas operated at 3000 volts potential difference with a leakage current of less than 0.003 milliampere. Minimum breakdown voltage was 4400 volts.

STAR Category 28

EXPERIMENTAL INVESTIGATION OF MERCURY PROPELLANT FEED ISOLATORS FOR KAUFMAN THRUSTERS

by Shigeo Nakanishi

Lewis Research Center

SUMMARY

An experimental investigation was conducted to evaluate the performance of seven high-voltage isolator configurations for a Kaufman ion thruster mercury propellant feed system. Defined for each configuration are the electrical breakdown voltage and the leakage current through the isolator over a range of propellant flow rates or pressure. Estimated gaseous pressure within the isolator was from 0 to 50 torr (0 to 1.07×10^3 (N/m^2)).

A configuration utilizing a long propellant flow passage and large recombination surface areas had a minimum breakdown voltage of 4400 volts. Maximum leakage current was below 0.003 milliampere at the nominal design voltage of 3000 volts.

An isolator containing 40 insulated segments experienced no breakdown up to the maximum applied test voltage of 5000 volts. Leakage current at 3000 volts was of the order of 0.10 milliampere.

It was concluded that a medium possessing large surface area is essential for reducing the leakage current and raising the electrical breakdown limit.

INTRODUCTION

Analytical and experimental studies of primary spacecraft propulsion systems using electrostatic thrusters have shown the advantages of the modular system concept (ref. 1). The advantages result from increased reliability and from the flexibility in power and load matching to conform to mission requirements and available solar power.

One requirement of the systems associated with the modular concept is reliable propellant distribution to each thruster from a common propellant tank. Another requirement is the ability to decouple each thruster module from the system electrically to permit standby status or total isolation in the event of a permanent fault. In ful-

filling these requirements, a propellant feed isolator is necessary.

Isolator designs capable of withstanding potential differences up to 10 kV at a gaseous pressure of 0.075 torr (1.6 N/m^2) have been reported in reference 2. These isolators were designed primarily for discharging mercury propellant vapor into a thruster using an oxide cathode. Estimated discharge pressures were of the order of 10^{-4} to 10^{-3} torr (2.13×10^{-3} to 2.13×10^{-2} N/m^2). The use of a hollow cathode in the Kaufman thruster (ref. 3), however, requires that the isolator be capable of operating over a pressure range from 0 to 50 torr (0 to 1.07×10^{3} N/m^2). The minimum pressure corresponds to the essentially no-flow condition of a start-up sequence. The maximum pressure is an estimated value to satisfy the flow requirements of both the cathode and the thruster ion chamber. Previous isolators, designed for low-pressure operation, were found to be ineffective at the higher pressures required for the present system.

An experimental investigation was conducted to evaluate several conceptual designs for a "high pressure" propellant feed isolator. Seven configurations were evaluated. High voltage breakdown limits and leakage currents through the isolator were determined as a function of propellant flow rate. The investigation was conducted in the test chamber of a 5-foot diameter by 16-foot long vacuum facility.

DESIGN REQUIREMENTS

Dimensional and Operational Constraints

A sketch of the 15-centimeter-diameter Kaufman thruster designed for the SERT II (Space Electric Rocket Test II) flight is shown in figure 1. Details of this thruster, which produces a 0.25 ampere beam current at 3000 volts, is described in reference 3. The isolator is mounted as an integral part of the thruster assembly, thus imposing certain dimensional constraints. The length of the isolator is limited to approximately 5 centimeters. The outside diameter is nominally 2 centimeters.

The isolator must be capable of handling up to 0.3 equivalent amperes (or 3.1×10^{-6} mole/sec) of mercury vapor propellant flow. This includes the flow to the cathode and the thruster distributor. The gaseous pressure corresponding to this flow rate is estimated at a maximum of 50 torr (1.07×10^{3} N/m^2). The total cross-sectional area of the discharge holes in the isolator and in the cathode tip is very small compared with the flow passage cross-sectional area of the isolator. The pressure drop across the isolator is thus expected to be a negligible fraction of the prevailing gaseous mercury pressure.

Electrical leakage through the isolator may occur as a nonluminous Townsend discharge. These leakage currents should be held to a minimum, possibly 10 micro-

amperes or less, to minimize power losses and any long-term progressive deterioration.

The operating temperature is limited to between 250° and 300° C. The upper temperature limit is based on considerations such as thermal feedback to the vaporizer and excessive heat loss due to radiation. The lower temperature limit is slightly in excess of the equilibrium temperature of 235° C for mercury vapor at 50 torr (1.07×10^3 N/m^2).

Design philosophy. - A possible basis of design is the Paschen curve of electrical breakdown for mercury vapor defined usually for a uniform field gap. A composite Paschen curve drawn from references 4 and 5 is shown in figure 2. A minimum breakdown voltage of 400 volts occurs at a pd value of 0.7 torr centimeter (14.9 (N/m^2)(cm)). To the left of this minimum, high breakdown voltages at high gas pressures require gap dimensions which are too small to maintain in practice. To the right of the minimum breakdown point, at the design voltage of 3000 volts, the gap required is about 1 centimeter for the maximum expected pressure of 50 torr (1.07×10^3 N/m^2). At lower pressures the required gap becomes even greater if a sufficiently large value of pd is to be maintained. Thus, these gap requirements appear to be mutually exclusive over the pressure range to be encountered.

The difficulties outlined above preclude a straightforward design approach, and two concepts were used as guidelines to arrive at a workable configuration. One concept is to grade the total voltage over numerous increments or segments so that each segment is subjected to a potential difference less than the minimum breakdown voltage. Ideally, no segment will reach the minimum breakdown voltage of 400 volts, and as few as 10 segments at 300 volts each will support 3000 volts. An equal voltage increment can be obtained across each segment by means of an externally applied linear voltage gradient. Background ionization may occur, however, and any flow of leakage current must be sufficiently low so that excessive heating or distortion of the voltage gradient does not occur.

A second design concept is to provide a combination of long path length and large recombination surface area in an extension of techniques described in reference 2. With the long path length, high values of pd and breakdown voltages are obtained at high gas pressures as indicated by the right-hand side of the Paschen curve. At lower pressures, leakage current and the occurrence of secondary processes which lead to a breakdown may be inhibited by providing large surface areas in the propellant flow passage. Charged particles believed to be instrumental in the formation of a breakdown discharge are restricted in motion or are lost at the surfaces via recombination.

Of the seven isolator configurations described in the APPARATUS section, the graded voltage types were evaluated first to determine their design requirements and performance limitations. Specific designs to incorporate the second concept then evolved with the progress of the evaluation tests.

APPARATUS

Feed System and Cathode Assembly

Those features of the thruster system incorporated into the test apparatus are shown schematically in figure 3. The propellant feed system consisted of a liquid mercury reservoir, shutoff valve, and a glass capillary tube flow rate meter. Mercury vapor from an electrically-heated porous tungsten vaporizer was passed through the isolator and fed to a hollow cathode. Most of the components and circuitry for the cathode assembly are identical to those of the SERT II thruster and a detailed description may be found in reference 3. Briefly, the cathode assembly consisted of a hollow cathode, keeper electrode, and baffle surrounded by a cylindrical magnetic field pole piece (not shown) mounted on a boron nitride disk to maintain proper positioning. The cathode was made of 0.32 centimeter diameter tantalum tubing with a 0.1-centimeter-thick disk of 2 percent thoriated tungsten welded on the end. A nominally 0.02-centimeter-diameter hole in the disk forms the cathode aperture. The cathode is heated by a tungsten rhenium wire coil encapsulated in flame-sprayed alumina and radiation shielded with layers of 0.012-millimeter-thick tantalum foil.

The keeper electrode is made of 0.15-centimeter diameter tantalum wire shaped into a 0.6-centimeter-diameter ring and positioned 0.2 centimeter from the cathode tip. As in thruster circuitry, the keeper bias supply had a load characteristic such that the output voltage dropped rapidly with increasing current.

The baffle, which is shown connected through a power supply, was normally held at the same potential as the cathode. The baffle and the magnetic pole piece were used primarily to provide a propellant flow configuration similar to that found in the cathode region of the thruster. No magnetic field was supplied to the pole piece.

The downstream end of the isolator and the cathode were connected to the positive output terminal of a high voltage direct current power supply. The negative output terminal of this supply was grounded. The upstream end of the isolator could be isolated or connected to ground through a leakage current meter by means of a grounding relay.

A photographic view of the isolator test apparatus is shown in figure 4. The isolator is shown mounted in the test compartment which, during test, was fitted with a glass bell jar and exhausted into the vacuum facility through a 12-inch gate valve.

Isolators

A view of a typical isolator assembly is shown in figure 5. The nonconductive isolator body was clamped between two stainless steel flanges 5 centimeters in diameter

and 0.46 centimeter thick. Clamping action was obtained by three ceramic terminal insulators fitted with screws.

The isolator assembly was heated by means of swaged heater elements wound around the periphery of the end flanges. To assure a uniform temperature distribution along the length of the isolator, several layers of tantalum foil were wrapped around the isolator taking precautions not to short the end flanges together electrically. A view of the disassembled isolator is shown in figure 6.

In all, seven isolator configurations were tested. Each isolator configuration was designed to conform to the fixed dimensions of the end flanges. Thus, in practice, each of the seven configurations was obtained by clamping the nonconductive element between the flanges and using ceramic cement and sealants to prevent propellant leakage.

In fabricating the various isolator configurations, bonding the components to produce a leak-tight assembly was difficult. The use of special brazing alloys for metal-to-ceramic bonding is a well-developed technology. Application of the technology to the present configurations, however, would have required considerable grinding or machining of ceramic pieces and fixturing of the assembly prior to the final brazing operation. In view of the many configurations and pieces involved, an expedient method of ceramic cementing and sealing was adopted. As a result, some propellant leakage was encountered with each configuration. Sufficient propellant pressure was obtained at the cathode, however, to permit its operation and a satisfactory evaluation of the performance of each isolator configuration.

Configuration A. - A drawing of a voltage-graded isolator is shown in figure 7(a). The two end flanges and one of the three insulator rods are drawn in their proper positions. The isolator body consisted of 15 aluminum oxide washers 0.32 centimeter thick with an outside diameter of 1.9 centimeters and an inside diameter of 0.875 centimeter. Each washer contained a piece of screening made of 0.077-millimeter stainless-steel wire woven in a plain square weave pattern. The screen was cemented to the inside diameter of the washer with high temperature insulating cement.

Baffles made from 0.038-centimeter-thick tantalum were sandwiched between the ceramic washers. Each baffle was provided with a connection terminal for wiring into a voltage divider resistor network. A 0.32-centimeter-diameter hole was drilled off-center in each disk and consecutive disks were oriented so that the holes were always 180° apart. The isolator body, consisting of a stacked assembly of 15 washers and 14 baffles, was clamped between the end flanges and coated with a layer of high-temperature ceramic insulating cement. After curing in a temperature-regulated oven for four hours, a second layer of cement was applied and cured. The cement exhibited some degree of porosity, and thus required two coats of a silicone-base vacuum sealant which was oven-cured for two hours.

The voltage divider network consisted of 15 resistors of 500 kilohms, each connected

in series between the end flanges of the isolator. The node points in the divider were connected to a rotary wafer-type selector switch to permit the voltage measurement of each segment of the isolator.

Configuration B. - A configuration containing 29 screens is shown in figure 7(b). It is essentially the same as configuration A except that the 14 tantalum baffles were replaced by pieces of densely woven tungsten screening. The screen consisted of 0.127-millimeter-diameter tungsten wire spaced 10 wires per centimeter. The cross wires were of 0.077-millimeter-diameter tungsten woven 120 wires per centimeter in a twill pattern. A notable property of this type of weave is that a through line of sight does not occur normal to the surface of the screen.

As before, the isolator body was coated and sealed, but no electrical connection was made to the segments.

Configuration C. - A 40-segment isolator configuration is shown in figure 7(c). The number of segments used was determined by taking into consideration the overall length requirement and the feasibility of maintaining close spacing between the baffle disks. The segments were formed by alternately stacking a baffle disk and an insulator spacer. The baffle disk was fabricated of 0.038-centimeter-thick tantalum, and was stamped with a circular ridge and an axial projection. A 0.32-centimeter-diameter hole was drilled at a radius of 1.78 centimeter and covered with a piece of the twill-weave tungsten screening described in configuration B. Consecutive baffles were oriented so that the drilled hole would be 180° apart. The spacing between baffles was maintained by a 0.076-centimeter-thick by 0.92-centimeter-outside-diameter boron nitride spacer. The spacer had a circular recess at the center into which the axial projection in the baffle fitted. This projection and the circular ridge held the boron nitride spacer in position.

A tantalum wire ring was spot-welded to each of the two end baffles. The ring was sized to fit inside the counterbored recess in the end flange, thus holding the isolator body concentric to the flange axis. The stacked assembly of baffles and spacers was clamped between the flanges, coated, and sealed as in the previous configurations.

Configuration D. - Figure 7(d) shows a labyrinth-type isolator which utilizes a long propellant flow passage and a large surface area to promote recombination. The isolator is longitudinally symmetrical about the midplane. Boron nitride was used in fabricating the end pieces and the caps because of its ease of machining. An aluminum oxide tube was cut to length to form the isolator body. A wad of tungsten wool having 0.0013-centimeter-diameter strands was packed at the midplane position to hold the end caps in place and to provide additional recombination surface. The propellant entered a drilled axial-flow passage in one of the end pieces. The flow followed a tortuous passage formed by the end cap and the outer tube, through the midplane tungsten wool pad, and retraced a similar pathway to exit at the axial passage of the downstream

end piece. Joints and mating surfaces were sealed by the same method used in the earlier configurations.

Configuration E. - As can be seen in figure 7(e), this configuration was identical with configuration D with the exception of two additional pads located within the end caps. The tips of the end pieces were sawed flat to provide the necessary space and contact with the tungsten wool pads.

Configuration F. - The concentric flow isolator shown in figure 7(f) was designed to have a maximum flow passage length and wall surface area. The concentric cylinders machined into the boron nitride end pieces were so located that they nested into each other. The outer envelope of the isolator was an aluminum oxide tube cut to the required length.

Propellant was introduced through a drilled passage at the axis. The flow was reversed in direction four times before being discharged axially at the downstream end of the isolator. The overall dimensions of this isolator were slightly greater than those of previous configurations. Because of the limited strength of boron nitride, a somewhat heavy wall thickness was used throughout. High-strength alumina should permit the sizing down of the isolator to the necessary dimensions.

Configuration G. - This isolator, shown in figure 7(g), differed from the previous configuration only in the addition of the tungsten wool pads. Four of the pads were located at the bottom of the concentric passages, and were conveniently held in position by the opposing ends of the concentric cylinders. The fifth pad was packed in the axial cavity at the discharge end of the isolator. Each pad was sized and packed to give an approximate density of 1.6 gram per cubic centimeter.

PROCEDURE

After all electrical connections were completed, the test compartment was evacuated and opened to the vacuum facility. The isolator body was brought to operating temperature (300° C) with the two end flange heaters. The cathode discharge was initiated by heating the vaporizer and applying a 300-volt starting potential between the cathode and the keeper electrode.

Propellant flow rate was controlled by adjusting the vaporizer temperature. After each new setting of vaporizer temperature, the feedline temperature was allowed to stabilize in order to avoid flow measurement errors caused by the thermal expansion or contraction of the mercury. Liquid mercury flow was metered by valving off the feedline from the reservoir and timing the falling rate of a capillary column.

As mentioned previously, the isolators were subject to different amounts of propellant leakage, depending on the construction and quality of seal. Calibration runs to

determine the actual flow to the cathode were made by connecting the cathode directly to the vaporizer (without isolator) and by mapping the voltage-current characteristics of the keeper electrode circuit for each level of metered propellant flow. A typical set of these characteristics is presented in appendix A, together with a brief description of the operational behavior of the hollow cathode.

During an isolator test run, the desired propellant flow rate to the cathode was established by adjusting the isolator input flow to obtain a particular cathode voltage-current characteristic curve. For ease of operation, the procedure of establishing the cathode flow rate was used only for the nominal design point, that is, about 0.04 equivalent amperes of neutral flow. Other flow rates were established by simply setting appropriate values of vaporizer temperature. At each temperature setting the voltage-current data of the cathode discharge was recorded and later correlated with the calibration curve.

Leakage current to ground through the isolator was measured for various thruster potentials at each propellant flow rate. The breakdown voltage corresponding to each propellant flow rate was determined by two different methods. In the gradual method, the grounding relay remained closed while the thruster potential was gradually raised until breakdown occurred. In the impulsive method, the thruster potential was preset to near the breakdown voltage before closing the grounding relay. The preset voltage was successively increased in increments until a setting was obtained at which closure of the switch resulted in a breakdown. Comparison of the breakdown limits obtained by the two methods for a given operating condition showed reasonable agreement.

Breakdown was defined in either of two ways: (1) a very rapid buildup of the leakage current to such a level that the overcurrent breaker of the power supply was activated, accompanied by a loss of high voltage, or (2) a high current discharge through the isolator, insufficient to activate the overcurrent breaker, but disproportionately higher than would be expected from an extrapolation of the leakage current-thruster voltage variation prior to the breakdown voltage. This type of breakdown was characteristic of the very low-pressure regime in some isolators. The variation in leakage current was sufficiently pronounced to define the breakdown limit in this manner without difficulty.

RESULTS AND DISCUSSION

Method of Data Presentation

For a given configuration, the gaseous pressure is a significant variable in the formation of an electrical breakdown. However, propellant flowrate was used as the primary variable because it is more conveniently measured than pressure. Even so,

additional complications arose because of propellant leakage which differed from one configuration to another.

The actual propellant flow desired through the cathode can be reproduced by using the cathode characteristics as described in appendix A. As a test on the sensitivity of this method, it was determined that for a propellant flowrate of 0.033 equivalent amperes, a 1-milliampere change in flow corresponded to about a 0.3- to 0.4-volt change in keeper potential which was nominally at 39 volts. A base flowrate J_{00} for a particular isolator-cathode assembly, including leakage flow, can thus be defined as the metered input flowrate for which the cathode operates at a keeper potential of 39 volts and a keeper current of 0.5 ampere. The various propellant flowrates were then expressed as the ratio of the metered flowrate J_0 at any other condition, to the base flowrate J_{00}. By this method, relative gas pressure in the isolator could be estimated even at propellant flowrates below the operating limit of the cathode. It was assumed that the propellant leakage out of the isolator was proportional to the total propellant flow J_0 for flows other than the base flowrate.

The performance parameters to be presented as a function of the propellant flow ratios are the electrical breakdown voltage and the leakage current to ground. The breakdown voltage is the upper thruster voltage limit above which operation is not possible. The leakage current is presented for incremental levels of thruster potential and for the breakdown threshold when obtainable. Inasmuch as the leakage current during a breakdown or incipient breakdown is not a stable current, the current shown in some instances may be for voltages 100 to 250 volts lower than the actual breakdown voltage.

Isolator Performance

A summary table showing the relative performance results of the seven isolator configurations is presented in table I. The minimum breakdown voltage was not explicitly determined for every configuration. In some cases, therefore, the voltage was estimated from faired curves. Also tabulated are the range of breakdown voltages and the corresponding range of propellant flow ratios investigated.

Not all configurations were tested over the same range of variables. The leakage currents of each configuration, therefore, are approximate values obtained over the range covered for that configuration. The base point leakage current is the current obtained at a thruster potential of 3000 volts and the base propellant flowrate. The operational characteristics of each configuration are discussed in detail in the subsequent sections.

Configuration A. - Voltage measurements at the node points of the resistor network

for the voltage-graded isolator at a thruster potential of 3000 volts showed a linear voltage gradient of about 230 volts per segment across 14 segments. The 15th segment was at the same potential as the downstream isolator flange and thus field free. For two levels of propellant flowrates, no difference in the voltage gradient was observed. Performance data obtained with this configuration is shown in figure 8(a). Breakdown voltages above 3000 volts were obtained at very low propellant flow ratios and again at a flow ratio beyond an apparent minimum. It is believed that the minimum in the breakdown voltage curve is analogous to the minimum breakdown voltage in the Paschen curve. The comparison is only qualitative, inasmuch as neither the gaseous pressure nor the characteristic distance is defined for the isolator configuration.

As shown by the upper curve of figure 8(a), the leakage current ranged from 0.082 to 0.188 milliampere. Separate measurements at a thruster potential of 3000 volts showed the leakage current through the isolator to be about 0.60 of the leakage current through the resistor network. The relatively high current through the isolator was indicative of a gaseous discharge which occurred even though the potential between the segments was below the 400 volts minimum breakdown voltage of the Paschen curve for mercury. The existence of a discharge was further substantiated upon disassembly of the isolator segments. In each of the fine mesh screen interposed between the segment baffles, a hole was burned through, directly in line with the drilled propellant passage hole of the baffle.

Configuration B. - The performance of the isolator with 29 screens is shown in figure 8(b). In comparison with configuration A, breakdown voltages below 3000 volts occurred over a slightly narrower range of propellant flow ratios (or isolator pressure). The minimum breakdown voltage was only slightly higher than that of configuration A, but it occurred at about the same propellant flow ratio.

The leakage current at 3000 volts was of the order of 0.033 to 0.045 milliampere, depending on the propellant flow ratio. The absence of an externally controlled voltage gradient does not appear to be detrimental. Rather, the leakage current and the breakdown voltage appear to be more a function of the ionization and recombination processes occurring within the isolator. The relatively high level of leakage current again points to the existence of a gaseous discharge under some operating conditions. Examination showed burned holes in the stainless steel screening and evidences of high temperatures such as discoloration in the tungsten screening.

Configuration C. - The configuration containing 40 baffled segments operated without a breakdown up to 5000 volts which was the output voltage limit of the power supply. As defined previously, breakdown is a rapid avalanche-type buildup of leakage current culminating in an overcurrent trip of the power supply circuit breaker or a disproportionate rise in steady-stage leakage current with applied voltage. The close spacing of the baffles (0.012 cm) corresponds to a breakdown parameter of 0.7 torr centimeter

(14.9 $(N/m^2)(cm)$) for a minimum breakdown voltage of 400 volts per segment at a gaseous pressure of 58 torr (1.24×10^3 N/m^2). Any lower gas pressure should then result in a higher breakdown voltage per segment. Actually, a 10-segment configuration should sustain 3000 volts with a 1000-volt margin of safety, but such a configuration was not investigated because of the magnitude of the leakage current.

The total leakage current to ground through the isolator consists of two components, a gaseous leakage current and an isolator body leakage current. In operation, these components cannot be metered separately. To obtain the net, or gaseous leakage current, the isolator was first operated at a given temperature with no propellant. The body leakage current thus measured was assumed constant when propellant was flowing and the value was subtracted from the total metered leakage current. The result is the net leakage current plotted in figure 8(c).

At a propellant flow ratio of 0.165, the total measured current was about equal to the body leakage current. Further reduction in propellant flow was characterized by the same variation in leakage current with applied voltage indicating that the measured current was essentially the isolator body leakage.

Although no breakdown was encountered, the leakage current, particularly at a propellant flow ratio of 1.0, was unacceptably high. No internal damage was sustained because refractory metal was used for the baffles and the screening. Also, the tests were conducted with a minimum of operating time at high leakage current conditions. It is believed that reducing the number of segments would result in higher leakage current through both the isolator passage and the body. Heat thus generated could eventually cause a thermal runaway condition in the insulator material.

Configuration D. - This isolator configuration marked a departure from the multisegmented-voltage-graded approach to a concept utilizing a long propellant passage length and adequate recombination surface area. As can be seen in figure 8(d), this design approach significantly narrowed the range of propellant flow ratios at which breakdowns below 3000 volts occurred. The breakdown limit increased rapidly from a minimum of 2500 volts. The leakage current was also an order of magnitude lower than that obtained in the multisegmented configurations. At a given thruster potential, the leakage current generally increased slightly with propellant flow or pressure. Apparently, the long passage length reduced the tendency toward high gaseous pressure breakdowns in analogy to the right side of the Paschen curve. In the region of low pressure, techniques developed in reference 2 appear to be applicable.

Configuration E. - The performance results of this configuration served to evaluate the effects of additional surface area as a result of the addition of the tungsten wool pads. It can be seen in figure 8(e) that the breakdown voltages were not significantly affected. Leakage current during stable, steady-state operation was reduced approximately to one-half that obtained in the same isolator using only one tungsten wool pad. From a

breakdown standpoint, it appeared that improvements in the high voltage isolation should utilize longer passages rather than simply increasing the number of pads. The validity of this conclusion was subjected to test in the following two configurations.

Configuration F. - As shown in figure 8(f), the performance of the concentric flow isolator without the tungsten wool pads was significant for its inability to sustain voltages above 3000 volts over a broad range of propellant flow ratios. The minimum breakdown voltage was reduced to 2000 volts. Even at high propellant flows, 4000 volts was sustained only with difficulty.

The leakage current at a thruster voltage of 1000 volts was lower than that of any previous configuration. At higher voltages, however, the leakage current increased and became erratic at the lower propellant flow conditions. These are indicated in the figure by data points connected by vertical bars. Currents measured on the panel meter fluctuated between these extreme values. The fluctuations had the characteristics of currents spike, and the accuracy of the indicated upper value is in doubt because of the meter damping. The upward fluctuation was generally accompanied by a visible blue flash that appeared to be within the outermost passage of the isolator. Because of the slightly translucent quality of the aluminum oxide tube used, it was possible to note the difference in the visible discharge characteristics at breakdown. In the high-pressure or high-propellant-flow ratio regime, the breakdown was accompanied by a single continuous flash which lasted until the over-current circuit breaker in the power supply opened. In the flow regime where erratic fluctuations in the leakage current occurred, the visible flash was intermittent. If the discharge was self-extinguishing before the circuit breaker opened, voltage was sustained. A sufficiently high current spike caused the circuit breaker to open. These intermittent discharges were aperiodic. In the very low pressure regime, the transition from steady-state to breakdown was more gradual. The nature of the breakdown was similar to that of a continuous visible glow discharge. Although the leakage current increased markedly at onset, the circuit breaker seldom opened because the steady-state current did not exceed the trip limit.

The conclusions to be drawn from these results are that passage length alone is not sufficient to obtain high voltage isolation. The tortuous flow path also provides a large wall surface area of dielectric material, but its ability to prevent cumulative ionization or the buildup of the secondary process preceding a breakdown appears limited.

Configuration G. - The performance of this configuration shown in figure 8(g) surpassed all others. The minimum breakdown voltage of 4400 volts occurred at a propellant flow ratio of about 0.14. At flow ratios below 0.09 and above 0.3, the breakdown voltage was in excess of 5000 volts and undetermined because of the output voltage limit of the power supply. A thruster startup and shutdown sequence was simulated with 3000 volts maintained across the isolator. No breakdown or leakage current transient was encountered. With an applied voltage of 3000 volts, the maximum leakage current

was about 0.003 milliampere at a propellant flow ratio in excess of 2.0. Current spikes and erratic leakage currents were obtained at voltages near the breakdown minimum. As in the previous configuration, the current spikes were accompanied by transient discharges visible through the isolator body.

The concentric flow configuration with five tungsten wool pads, fulfilled the design requirements in all respects. A flight design would probably be fabricated from high-strength alumina with some possible reduction in overall dimensions. The interchangeable flange construction would be replaced with permanently brazed end caps.

Although the performance of the present configuration is acceptable, it is assumed that some degree of optimization is possible. For example, the number, density, and relative positions of the several tungsten wool pads can be varied. Use of a high surface area medium other than tungsten wool may be desirable. A considerable amount of electrical heating power was required to maintain an isolator body temperature of 300^{o} C. This is attributed to the large amount of exposed radiative surface area. A test showed that a minimum surface temperature of about 210^{o} C was tolerable before a noticeable change in the cathode discharge characteristics occurred because of propellant loss due to condensation within the isolator. A partially enclosed mounting design plus heat shielding should favorably reduce the heating requirements.

CONCLUSIONS

An experimental investigation was conducted to evaluate seven isolator configurations for the mercury propellant feed system of a Kaufman thruster. In one case, an isolator containing 40 insulated segments formed by closely spaced baffles with staggered passage holes withstood voltages in excess of 5000 volts. Leakage current at 3000 volts, the design voltage, was of the order of 0.10 milliampere. Grading the potential difference across the isolator in 15 equal increments did not obtain the anticipated value of breakdown voltage.

A minimum breakdown limit of 4400 volts was obtained for an isolator utilizing a long flow passage in a labyrinth-type concentric arrangement and five tungsten wool pads. At propellant flowrates other than the value at the minimum, the breakdown voltage was in excess of 5000 volts. Maximum leakage current through the isolator at 3000 volts was of the order of 0.003 milliampere. The leakage current generally increased with propellant flowrate or pressure. The identical concentric-flow configuration without the tungsten wool pads was capable of withstanding a minimum voltage of 2000 volts.

It is concluded that a medium possessing a large surface area is essential for reducing the leakage current and raising the electrical breakdown limit. The best of the

configurations tested could probably be improved further in terms of performance, durability, and eventual flight application.

Lewis Research Center,
National Aeronautics and Space Administration,
Cleveland, Ohio, February 28, 1968,
120-26-08-06-22.

APPENDIX - OPERATIONAL CHARACTERISTICS OF HOLLOW CATHODE

The current-voltage characteristics of the hollow cathode used in the investigation are shown in figure 9. Each curve was generated by adjusting the vaporizer temperature to obtain a constant metered propellant flowrate. For these tests, the vaporizer was connected directly to the cathode so that the indicated propellant flowrates are the actual flowrates through the cathode (i. e., no isolator leakage flow).

All of the components that immediately surround the cathode in an actual thruster were included in these tests. Not included, however, was the ion chamber itself and the main propellant flow. Normally, about 10 percent of the 0. 3 equivalent ampere of total propellant flow is fed to the cathode itself. The remainder is introduced into the ion chamber from distributor ports outside the magnetic pole piece surrounding the cathode (see fig. 1). The magnetic field within the ion chamber does not strongly affect the cathode characteristics. The presence of an ion chamber discharge plasma does, however. For example, a typical hollow cathode in a thruster operates at a keeper current of 0. 3 ampere and a keeper voltage of 13 volts. It can be seen from the curve for the 0. 033 ampere propellant flowrate that in the absence of an ion chamber discharge, the keeper voltage in the test setup was in excess of 30 volts.

A propellant flowrate of 0. 010 ampere was near the minimum for stable operation. As the curve for 0. 010 ampere flow shows, the keeper current had an upper limiting value regardless of the keeper voltage. Further reduction in propellant flowrate was characterized by a reduction in the keeper current and a quenching of the cathode discharge. At very high propellant flow rates, the keeper current was independent of keeper voltage.

In utilizing the cathode characteristics to establish the base flow rate J_{00}, a keeper current of 0. 5 ampere was selected. At this keeper current level, the mercury propellant flow-voltage characteristics are fairly reproducible. It can be seen from figure 9 that a current level of 0. 4 ampere can also be used, but with some sacrifice in sensitivity.

REFERENCES

1. Kerrisk, D.J.; and Kaufman, H.R.: Electric Propulsion Systems for Primary Spacecraft Propulsion. Paper No. 67-424, AIAA, July 1967.

2. Nakanishi, Shigeo: Experimental Investigation of a High-Voltage Isolation Device for Ion-Thruster Propellant Feed. NASA TN D-3535, 1966.

3. Kerslake, William R.; Byers, David C.; and Staggs, John F.: Sert II Experimental Thrustor System. Paper No. 67-700, AIAA, Sept. 1967.

4. Guseva, L.G.: Initiation of a Discharge in Molecular Gases at $pd < (pd)min$. Research in the Field of Electric Discharges in Gases. B.N. Klyarfel'd, ed., All-Union Institute of Electrical Engineering, Trans. (USSR), no. 63, 1958, pp. 1-38. (John Crerar Library Translation No. SLA 60-19079; also as Rep. No. MCL-3631V, Tech. Information Center, MCLTD, Wright-Patterson AFB, Ohio.)

5. Von Engel, Alfred H.: Ionized Gases. Oxford University Press, 1955.

TABLE I. - PERFORMANCE OF HIGH VOLTAGE PROPELLANT FEED ISOLATORS

Configuration	Type	Minimum breakdown voltage, V	Breakdown voltage range, V	Range of propellant flow ratio, J_0/J_{00}	Leakage current, mA (a)	Leakage current at base flow rate, mA (b)
A	15 Segment; voltage graded	2000	4000 to 3200	0.038 to 0.275	0.085 to 0.188	Not obtained
B	29 Screens	2200	3000 to 3800	.1 to 1.5	.01 to 0.06	0.037
C	40 Segments	None	None	.165 to 1.0	0 to 0.145	.097
D	Labyrinth ends; 1 pad	2550	5000 to 5000	.09 to 0.9	.0015 to 0.0165	.09
E	Labyrinth ends; 3 pads	2700	5000 to 5000	.08 to 1.9	.001 to 0.005	.0042
F	Concentric flow; no pads	2000	5000 to 4000	.117 to 4.0	.0005 to 0.02	.007
G	Concentric flow; 5 pads	4400	5000	.09 to 3.6	.0002 to 0.02	.0022

[a]Approximate over operating range tested (steady state).

[b]At 3000 volts thruster potential.

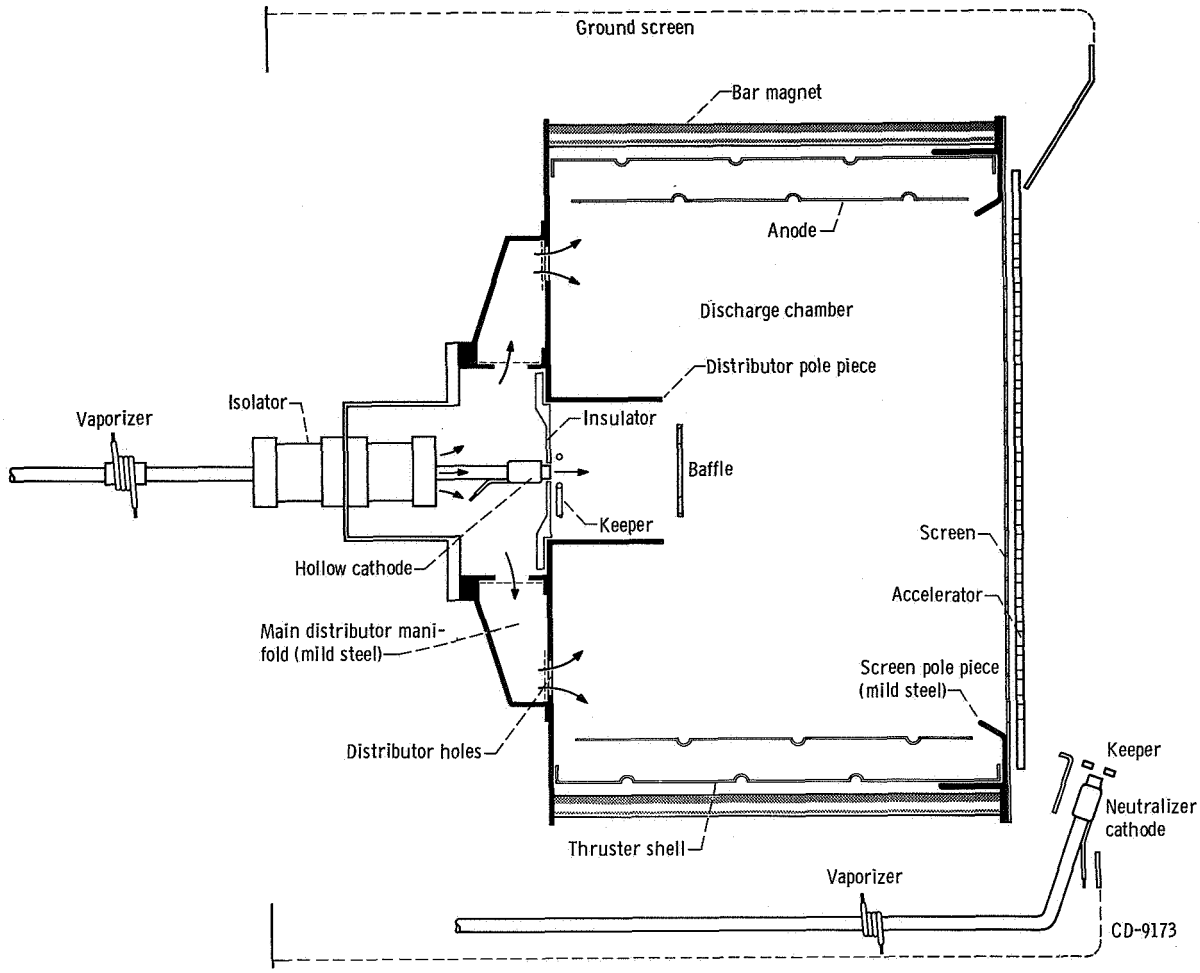

Figure 1. - 15-Centimeter diameter Kaufman thruster.

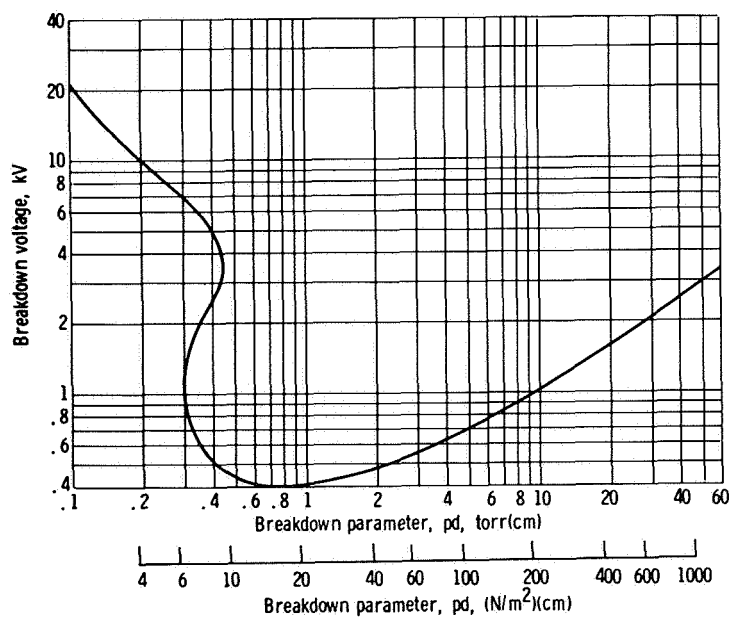

Figure 2. - Paschen curve for mercury vapor (refs. 4 and 5).

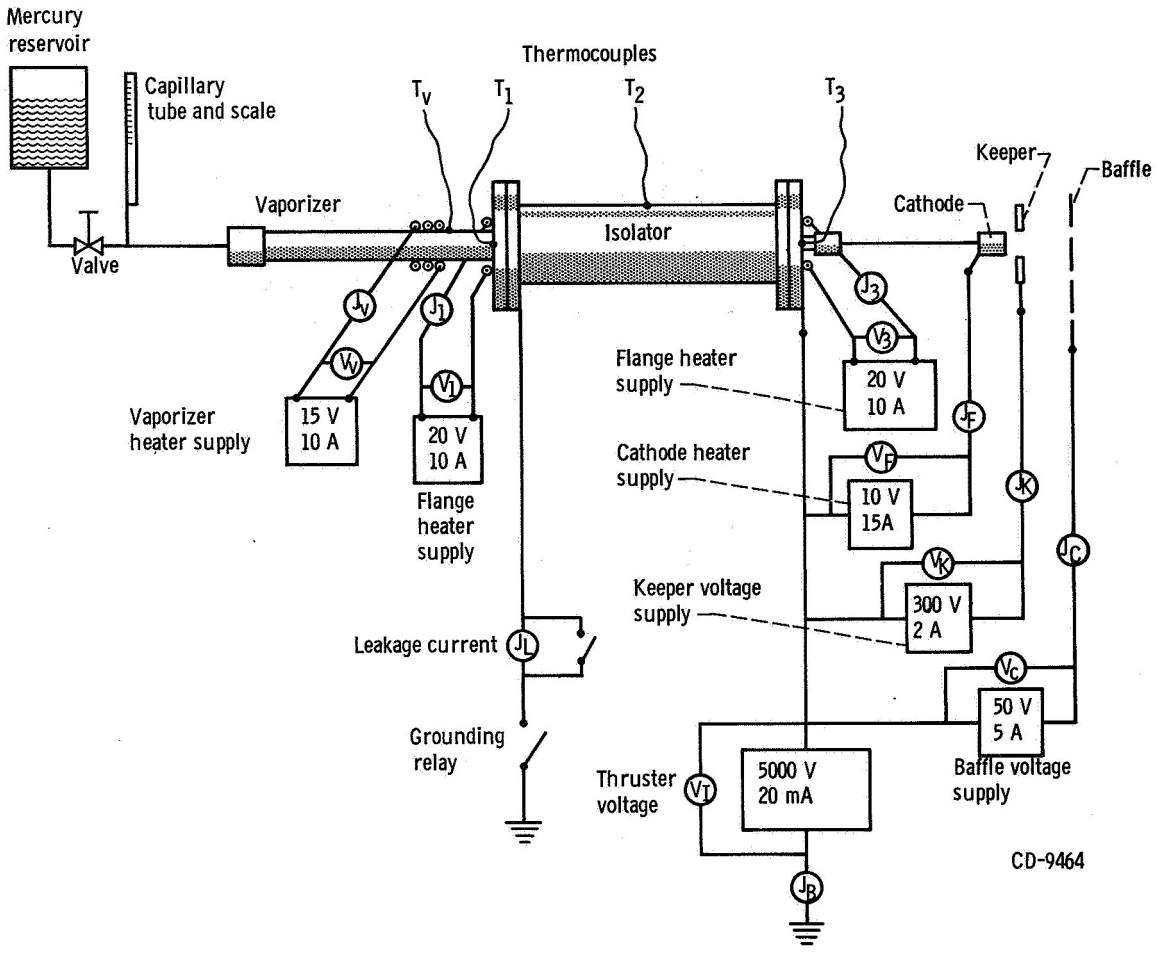

Figure 3. - Isolator test apparatus.

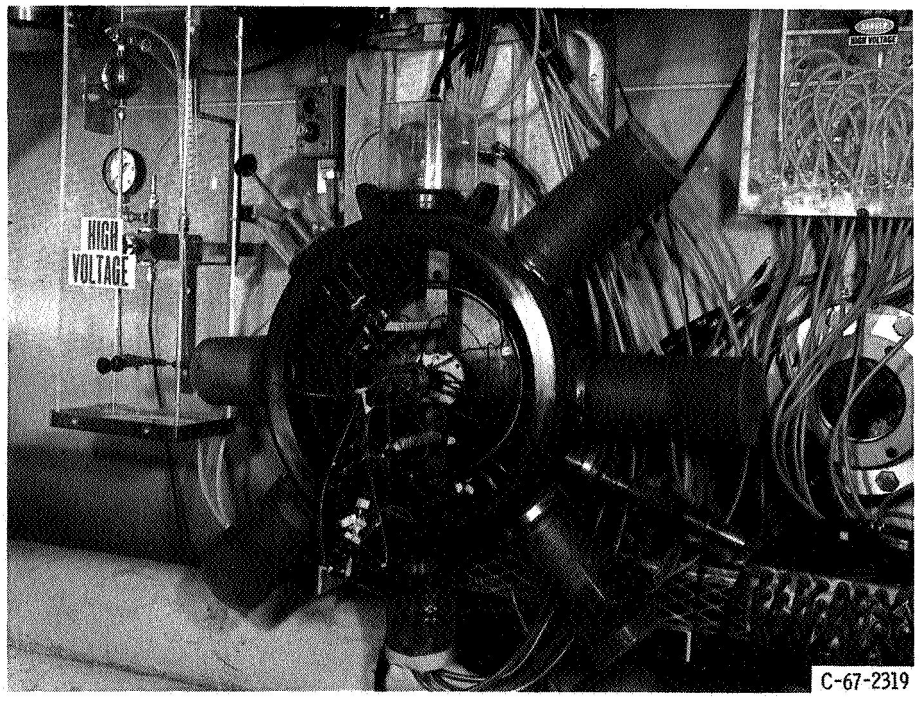

Figure 4. - Isolator apparatus in test compartment.

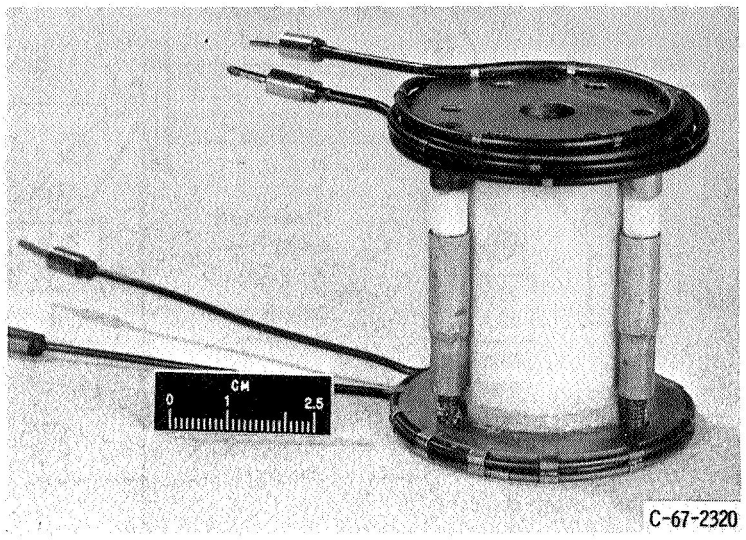

Figure 5. - Typical isolator.

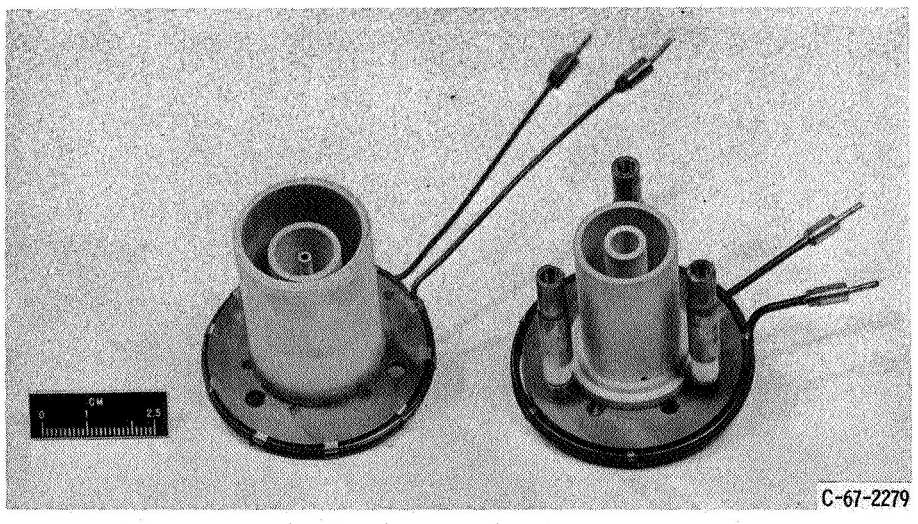

Figure 6. - Typical disassembled isolator.

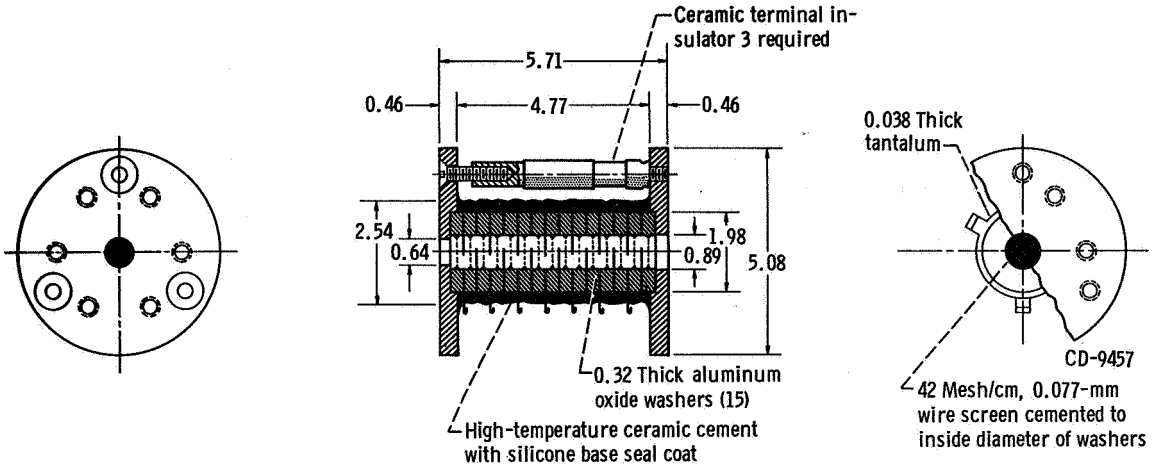

(a) Configuration A: Voltage graded.

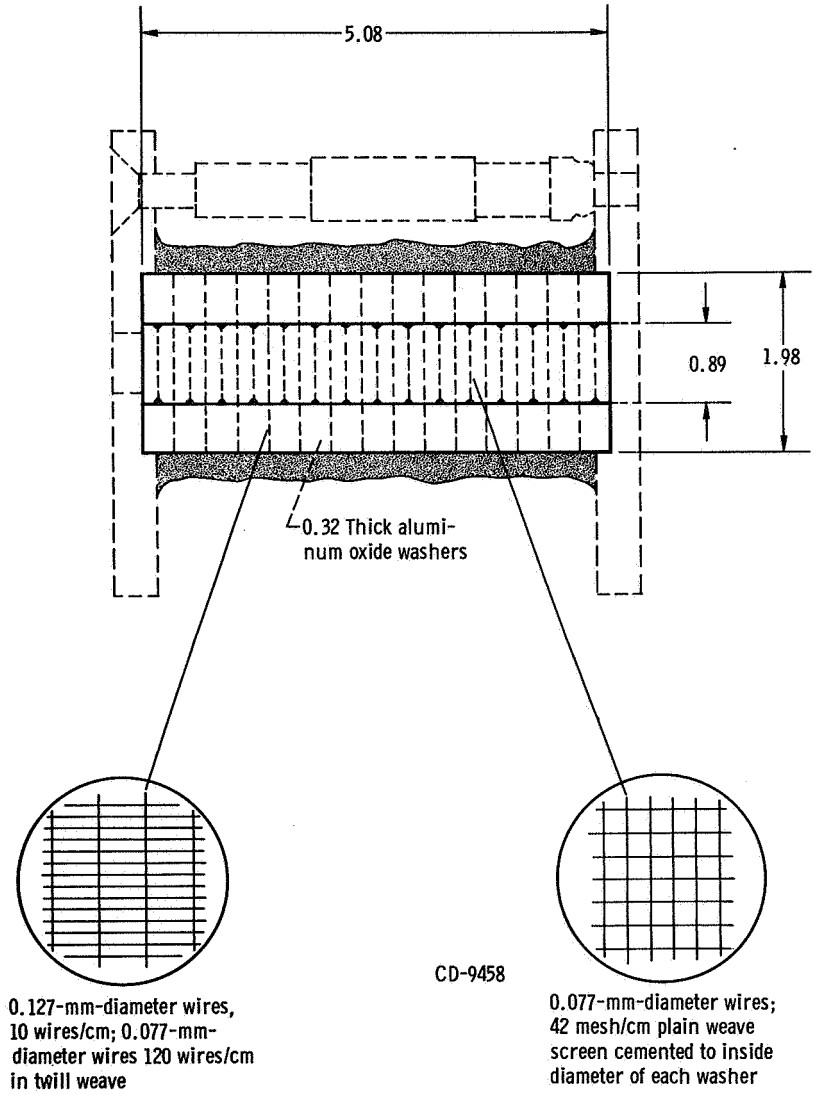

(b) Configuration B: 29 Screens.

Figure 7. - High-voltage propellant feed isolator. (All dimensions are in centimeters unless otherwise noted.)

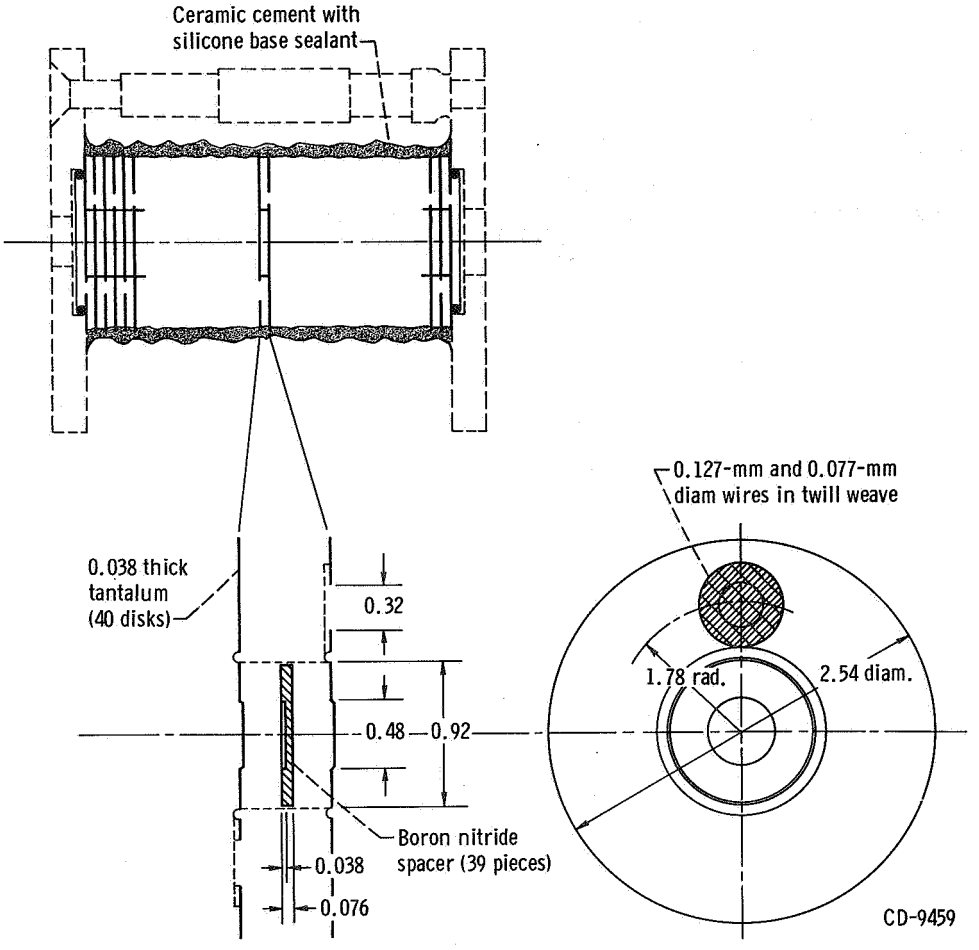

(c) Configuration C: 40 segments.

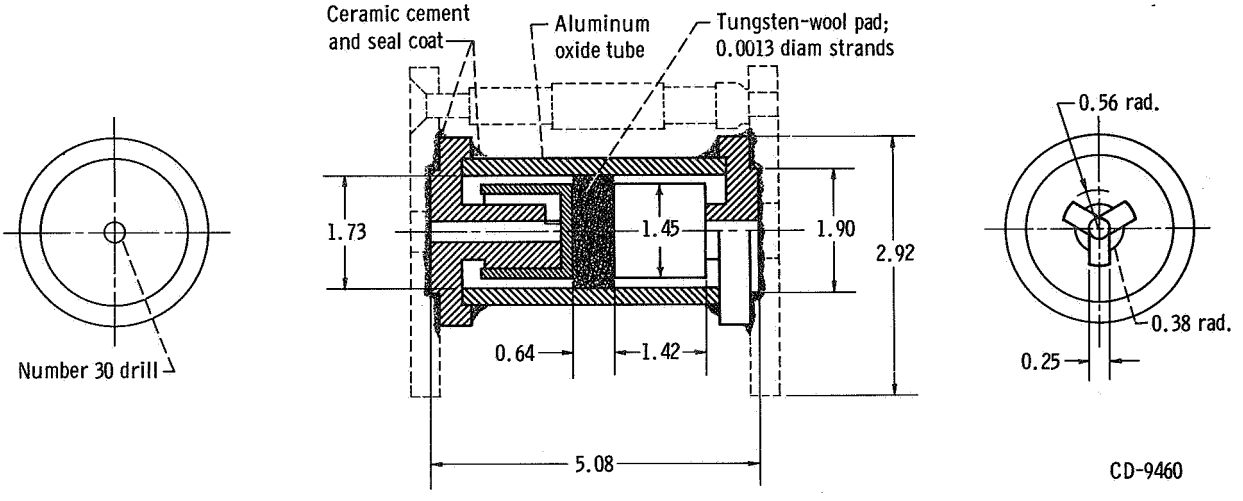

(d) Configuration D: Labyrinth ends, 1 pad.

Figure 7. - Continued.

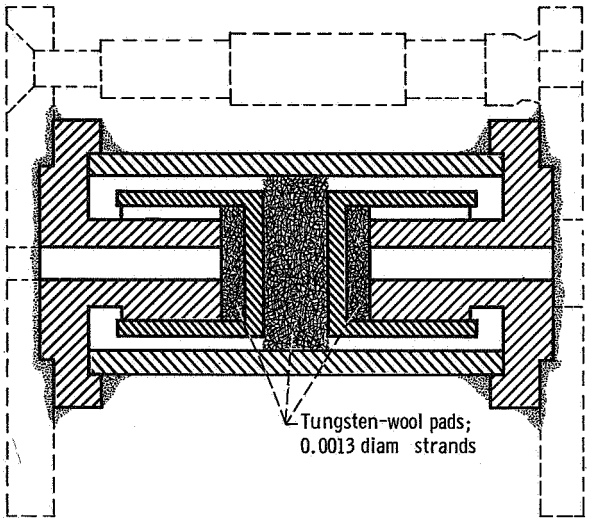

(e) Configuration E: labyrinth ends, 3 pads.

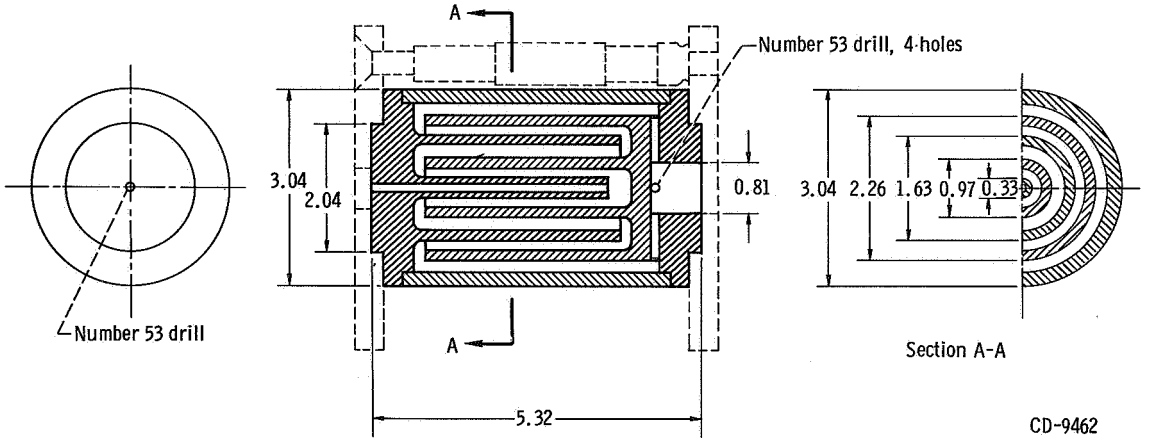

(f) Configuration F: concentric flow, no pad.

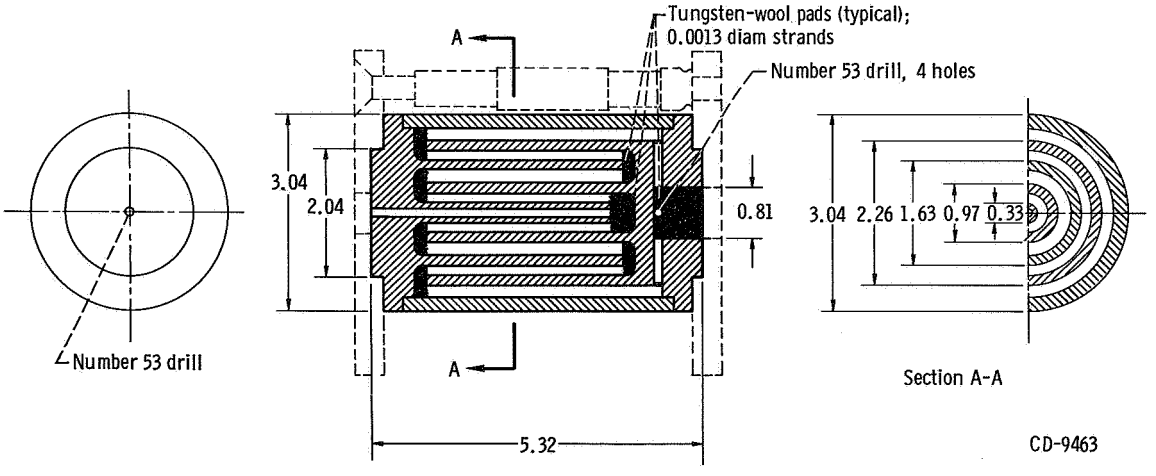

(g) Configuration G: concentric flow, 5 pads.

Figure 7. - Concluded.

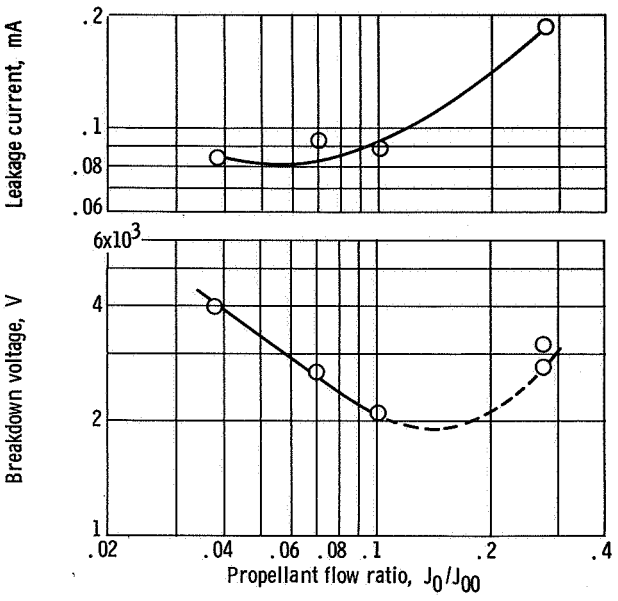

(a) Configuration A.

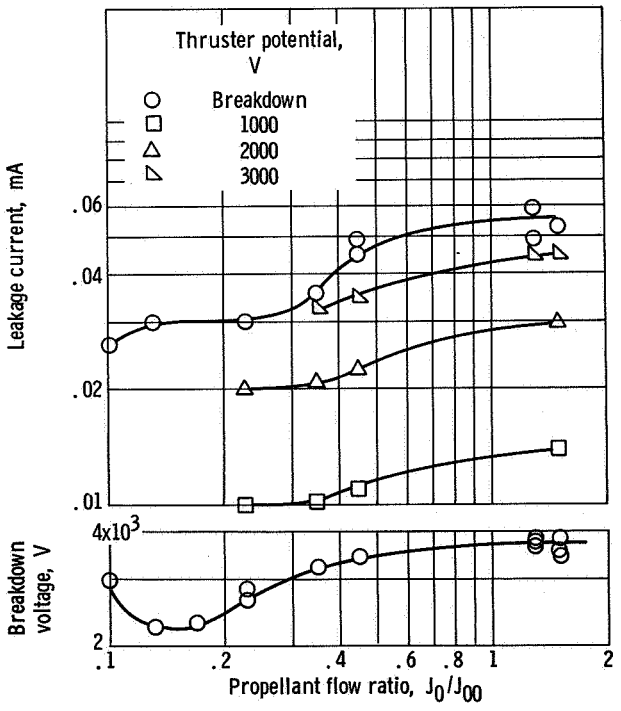

(b) Configuration B.

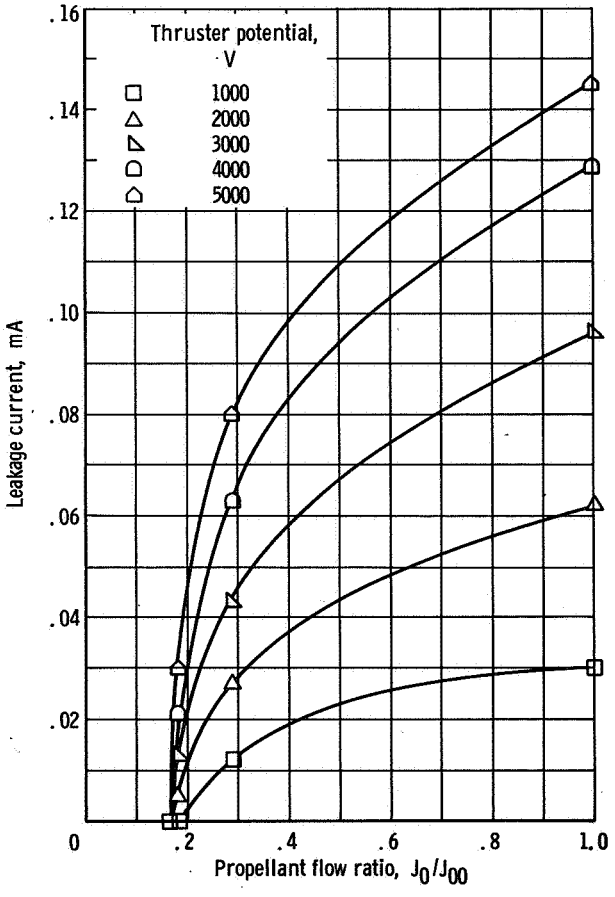

(c) Configuration C.

Figure 8. - Isolator performance.

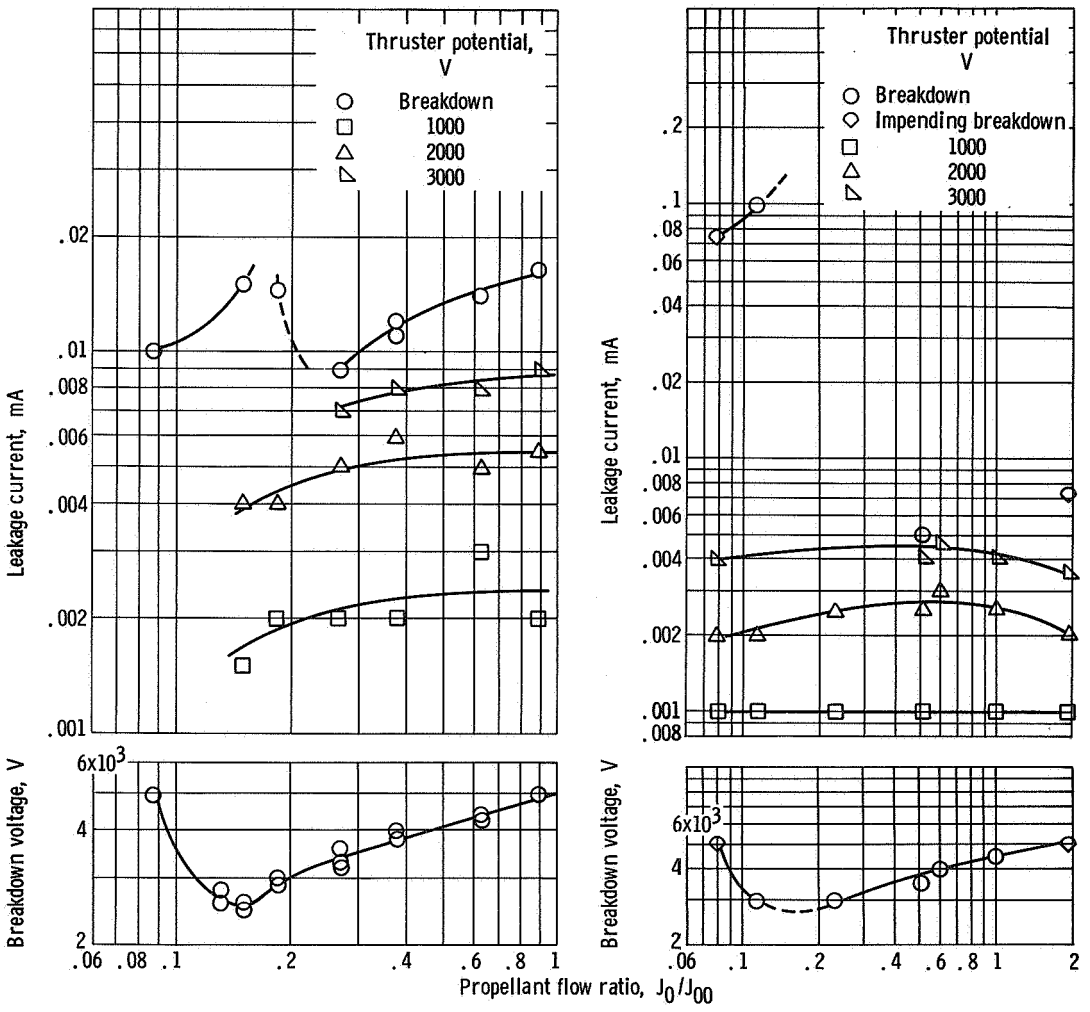

(d) Configuration D.

(e) Configuration E.

Figure 8. - Continued.

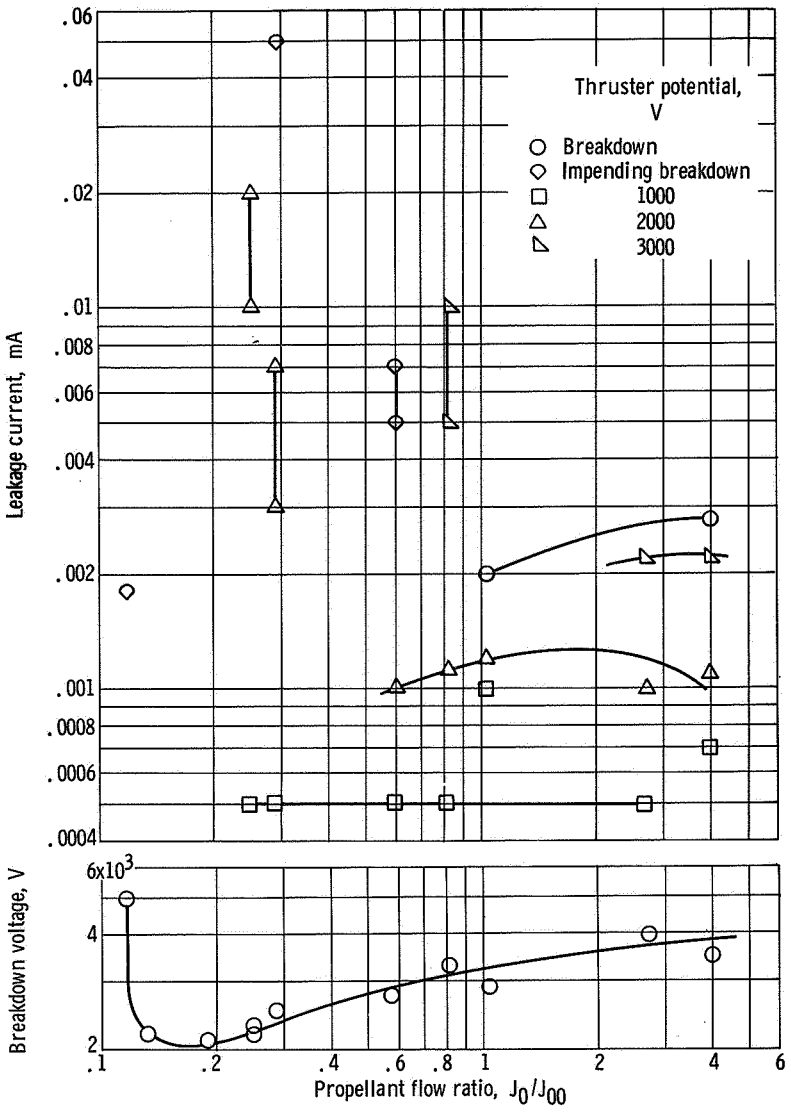

(f) Configuration F.

Figure 8. - Continued.

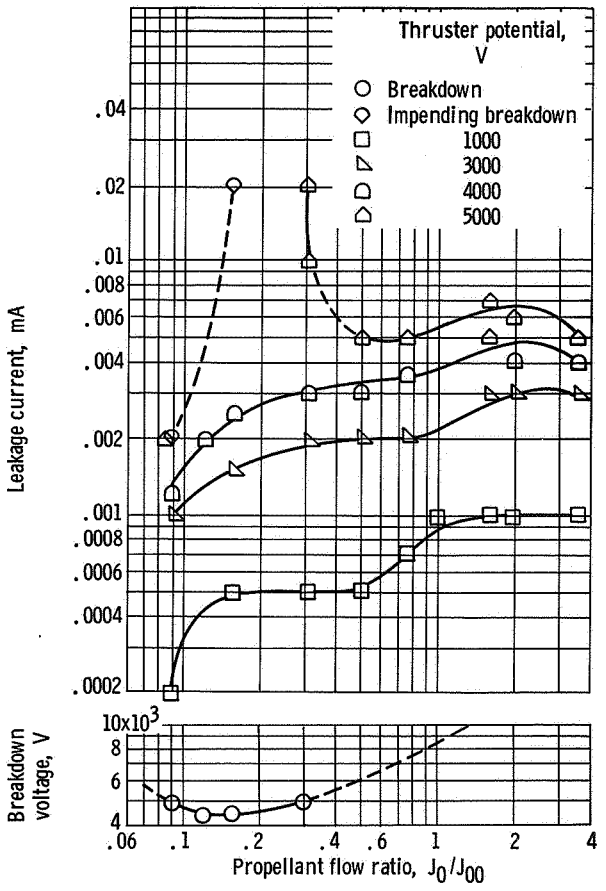

(g) Configuration G.

Figure 8. - Concluded.

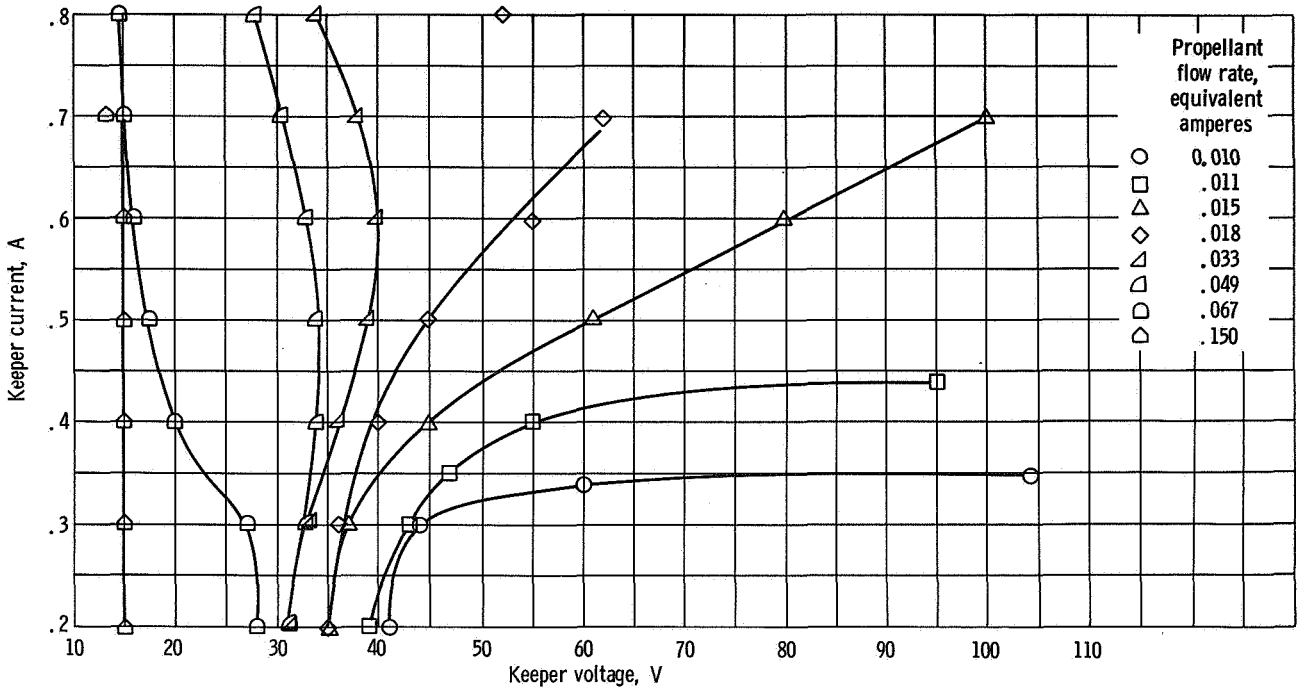

Figure 9. - Characteristics of hollow cathode.